ASIAN JOURNAL OF PHARMACEUTICAL AND CLINICAL RESEARCH

INNOVARE ACADEMIC SCIENCES
Knowledge to Innovation

Vol 19, Issue 4, 2026

Online - 2455-3891
Print - 0974-2441

Research Article

INTEGRATING GREEN CHEMISTRY AND QUALITY BY DESIGN: DEVELOPMENT OF A NOVEL STARCH-BASED MICROCOMPOSITE SYSTEM FOR PROLONGED CAPTOPRIL DELIVERY AND FLATTENED PHARMACOKINETICS

DINESH L BAWANKAR*, UJWAL B VYAS

Department of Pharmaceutics, Datta Meghe College of Pharmacy, Datta Meghe Institute of Higher Education and Research DMIHER (DU) Sawangi, Meghe Wardha, Maharashtra, India.
***Corresponding author: Dinesh L Bawankar; Email: dinesh.bawankar@gmail.com**

Received: 19 January 2025, Revised and Accepted: 02 March 2026

ABSTRACT

Objectives: The goal of this work was to form a new once-a-day oral dosage form (microcomposite beads) for the blood pressure drug Captopril that releases the medicine slowly, and that is built from a starch taken from plants by a low-impact "green" method.

Methods: Tubers of *Amorphophallus paeoniifolius* (Elephant Foot Yam) were the starting material. A deep eutectic solvent made from glycerol and choline chloride pulled the native starch, which was then carboxymethylated to produce Carboxymethylated Elephant Foot Yam Starch (CM-EFYS) with 0.45±0.03 carboxymethyl groups per glucose unit. Fourier-transform infrared spectra showed new carboxylate bands, X-ray data showed a 46.7% drop in crystallinity, while swelling power rose by 77% and solubility by 133%. A quality-by-design approach with a full factorial design-of-experiments matrix was used to prepare drug-loaded beads by combining CM-EFYS with sodium alginate and cross-linking in calcium chloride.

Results: The optimized formulation contained 3.2% w/v CM-EFYS, 3.1% w/v $CaCl_2$, and a polymer-to-drug ratio of 3.3:1, producing nearly spherical beads of 642±14 µm with 86.9±1.6% drug entrapment. The beads released Captopril gradually for 24 h and followed the Korsmeyer–Peppas model (R^2=0.992, n = 0.689). In rabbits, the beads reduced the maximum plasma concentration (C_{max}) by 62.2%, delayed time to C_{max} (T_{max}) from 2 h to 8 h, and increased mean residence time by 162.6%, while maintaining bioequivalent area under the curve. Six-month stability testing at 40°C and 75% relative humidity showed minimal potency loss when packed in foil.

Conclusion: A functional polymer for once-daily sustained release of captopril was successfully created from green-extracted, CM-EFYS. The optimized formulation demonstrated high drug entrapment efficiency (86.9±1.6%) and controlled 24-h release following Korsmeyer–Peppas kinetics (R^2=0.992, n=0.689). The formulation's stability under accelerated conditions demonstrated its potential as an efficient and environmentally friendly sustained-release oral dosage system.

Keywords: *Amorphophallus paeoniifolius*, Carboxymethyl starch, Deep eutectic solvent, Quality-by-design, Sustained release, Microcomposite beads, Captopril, Pharmacokinetics.

 DOI: http://dx.doi.org/10.22159/ajpcr.2026v19i4.58187. Journal homepage: https://innovareacademics.in/journals/index.php/ajpcr

INTRODUCTION

Oral tablets that let the drug seep out slowly have become a mainstay of present-day treatment. They steady the drug level in the blood, cut the number of daily doses and help patients stay on therapy for illnesses like high blood pressure (Adeleke, 2021). Among the materials used to build those tablets, natural plant sugars – especially starch – are favored because the body accepts them, they break down safely, they are cheap, and chemists can alter them in many ways (Masina *et al.*, 2017). Raw starch, however, dissolves too readily, swells too little plus crumbles too easily. To give it the right speed of release, chemists must change its structure (Kaur *et al.*, 2012). One common change is carboxymethylation – an ether reaction that clamps negatively charged carboxyl groups to the starch chains. The treated starch attracts water strongly, swells greatly, and forms a firm gel – it can be locked into a tablet by ionic cross-links and can respond to the pH of the gut (Tijsen *et al.*, 2001).

Many studies have used everyday starches from corn or potato, but researchers now look for lesser-known starches whose native structure might give better performance after the same chemical tweak. *Amorphophallus paeoniifolius*, the tropical tuber called Elephant Foot Yam, yields starch with a C-type crystal pattern but also a middle-of-the-range amylose-to-amylopectin ratio (Mishra *et al.*, 2019). This C-type lattice, a mix of A- and B-forms, takes up water and breaks down at a different rate from the patterns in common starches - after carboxymethylation, it could give a swelling and strength profile that suits prolonged release. So far, no one has tested this yam starch as a tablet ingredient. Recent studies have explored modified jackfruit (Narkhede *et al.,* 2011) and taro starches for drug delivery, demonstrating growing interest in non-conventional sources. However, *A. paeoniifolius* starch remains unexplored despite its unique C-type crystallinity.

Developing a dependable drug formula from new natural polymers needs a step-by-step plan that spots and lowers risk so the final product works every time Rathod *et al.,* (2025). The regulators back a method called quality-by-design (QbD). It starts – setting clear quality targets, studies the science behind the product plus builds controls into the process itself (ICH Q8 R^2). Teams first pick the key attributes of the finished drug, called critical quality attributes (CQA) then use designed experiments to tie those attributes to the properties of raw materials and to each machine setting. Once those links are known, the process can run inside a fixed "design space" but also still give the same result (Holler *et al.*, 2022).

The present work combined green chemistry, polymer science besides QbD into one continuous project. The main goal was to build a new once-a-day oral form of Captopril that releases the drug slowly using beads made from two polymers – alginate and a modified form of *A. paeoniifolius* starch that carries carboxyl groups (Carboxymethylated Elephant Foot Yam Starch [CM-EFYS]) Duchin *et al.* (1988). Five tasks

were set. Extract native EFY starch with a green deep eutectic solvent (DES) as well as convert it to the carboxymethyl form. Record how the starch changes in crystal pattern, shape, and flow after modification. Trap Captopril inside microbeads formed-dripping a polymer solution into calcium chloride, then improve the recipe through a QbD-designed experiment. Test how the drug leaves the beads in artificial gut fluid, how much crosses rat intestinal tissue, or how long the product stays within spec when stored. Run a head-to-head pharmacokinetic study in rabbits to prove that the beads stretch the time Captopril stays in blood. We expected that the added carboxyl groups would let the EFY starch swell and gel more than the native form, also that the alginate – starch mesh would slow the exit of Captopril in the test tube and hold the drug in the body for a longer period (Kaur *et al.* (2016)). The paper shows the full chain of steps, from green extraction of an unused tuber starch to animal data that support the idea of a once daily captopril dose.

MATERIALS AND METHODS

Materials

Fresh corms of Elephant Foot Yam (*A. paeoniifolius*) were acquired from the local marketplace of Bhandara, India, and authenticated by a botanist from the Department of Botany, Nagpur University (specimen no. 2025/178). Captopril (pharmaceutical grade, ≥98% purity) was a sample from Mylan Laboratories Ltd. Sodium alginate (medium viscosity, 2000 cps), choline chloride (≥98%), glycerol (≥99.5%), monochloroacetic acid (≥99%), sodium hydroxide pellets, calcium chloride dihydrate, isopropyl alcohol, and acetic acid were procured from Sigma-Aldrich.

Green isolation of native starch using DES

It was prepared using choline chloride and glycerol in a 1:2 molar ratio as described by Zdanowicz *et al.* (2018), with slight modification. Briefly, the components were heated at 80°C under continuous stirring (500 rpm) till a clear, homogeneous liquid formed. Fresh yam tubers were thoroughly washed, peeled, and cut into small cubes (1 cm^3). The cubes were homogenized with the pre-heated DES at a solid-to-liquid ratio of 1:5 (w/v, where "solid" refers to the weight of fresh tuber cubes in grams and "liquid" refers to the volume of DES in milliliters) using a high-shear mixer (Ultra-Turrax® T25, IKA, Germany; 10,000 rpm maximum speed, 24,000 min^{-1} maximum shear rate) at 10,000 rpm for 5 min. The homogenate was kept at 50°C for 2 h. It was shaken (150 rpm) on an orbital shaker. The resulting slurry went through centrifugation (Eppendorf 5810R Germany) at 3000 × g for 15 min. The liquid on top was thrown away. The starch at the bottom was mixed with 70% (v/v) ethanol. It was washed by spinning (3000 × g, 10 min) many times until the liquid on top was clear. The clean starch was dried in a forced-air convection oven (NSW-150, Narang Scientific Works India) at 40°C. It reached a steady moisture level (under 12% as measured by a moisture analyzer). The dry starch was crushed. It passed through a 100-mesh sieve. It was then kept in airtight containers at 4°C to use later.

Synthesis of CM-EFYS

Carboxymethylation carried out through an improved etherification method based on Tijsen *et al.* (2001). For a typical experiment, they suspended 50 g of native EFY starch in 250 mL of 85% (v/v) isopropyl alcohol in a reactor, reflux condenser, and thermometer. Then stirred the mixture at 200 rpm and added 25 mL of sodium hydroxide solution (30% w/v) over 30 min while keeping the temperature at 30°C Nataraj & Reddy (2020). The mixture then underwent alkalization for 60 min. After that, added 15 g of monochloroacetic acid liquified in 20 mL of isopropyl alcohol.

The temperature was then elevated to 55°C and maintained for 4 h with constant stirring. To end the reaction, they neutralized the mixture with glacial acetic acid to a pH of 6.5–7.0. Finally recovered the product by filtering it under vacuum, washed it in order with 80% ethanol, 95% ethanol, and absolute ethanol to get rid of sodium chloride, glycolate salts, and other by-products, and then dried it at 50°C for 24 h. They determined the degree of substitution (DS) using a non-aqueous acid-base titration method (Sang *et al.* 2020).

Briefly, 0.5 g of dried CM-EFYS was liquified in 25 mL of 0.1 M NaOH under stirring for 24 h. The surplus alkali was titrated against standard 0.1 M HCl, consuming phenolphthalein as an indicator. The DS was intended using the following equation:

$$DS=(0.162\times A)/(1-[0.058 \times A])$$

Where A is the milliequivalents of acid used up per gram of sample, 0.162 is the molecular weight of anhydro-glucose unit, and 0.058 is the net increase in the weight of anhydro-glucose unit per carboxymethyl group substituted.

The reaction yielded 41.2±2.1 g of CM-EFYS per 50 g of native starch (82.4%±4.2% yield). The final product was analyzed for residual isopropyl alcohol using gas chromatography (GC-FID) and was found to contain <100 ppm, well below the ICH Q3C limit of 5000 ppm. Chloride content, determined by argentometric titration, was 0.12%±0.02%.

Characterization of native and modified starch

The physicochemical properties of native and carboxymethylated starch (CM-EFYS) were evaluated using the following techniques: Fourier transform infrared (FTIR) spectroscopy spectra were recorded on a PerkinElmer Spectrum Two™ spectrometer (USA) in the range of 4000–500 cm^{-1} using the KBr pellet method to identify functional groups Cu Kα radiation (λ = 1.5406 Å) at 40 kV and 40 mA was used to create X-ray diffraction (XRD) images. At a step size of 0.02°, scanning was carried out between 5° and 50° (2θ). The proportion of the total area to the crystalline peak region beneath the diffractogram was used to calculate the comparative crystallinity (%). A simultaneous thermal analyzer was used to conduct differential scanning calorimetry (DSC) and thermogravimetric analysis. Samples (3–5 mg) were heated under a nitrogen purge (50 mL/min) from 30°C to 300°C at a rate of 10°C/min for DSC. Samples were heated under nitrogen from 30°C to 600°C at a rate of 10°C/min for TGA. Using a Carl Zeiss EVO 18 scanning electron microscopy (SEM) (Germany), granule morphology was investigated using SEM. Relative crystallinity was calculated using DIFFRAC.EVA software (Bruker, version 4.2) by integrating the crystalline peaks (2θ=15°,17°,18°,23°) and amorphous halo... Viscosity was measured using a Brookfield DV-E viscometer (USA) with spindle No. 62 at 50 rpm (equivalent to a shear rate of 6.6/s), which falls within the validated range (5–100/s) for these starch dispersions.

Swelling power and solubility

It was determined at 65°C, 75°C, and 85°C in distilled water and simulated intestinal fluid (SIF, pH 6.8 phosphate buffer) using the standard method (Leach *et al.*, 1959). Aqueous dispersions (5% w/v) were prepared, and the viscosity was measured using a Brookfield DV-E viscometer (USA) with spindle No. 62 at 50 rpm and 25°C.

QbD-based formulation development

This framework is particularly advantageous for natural polymers like starch, which exhibit inherent batch-to-batch variability in properties such as viscosity, particle size, and swelling behavior. QbD helps establish a robust design space that accommodates this variability while ensuring consistent product quality Verma et al. (2009).

Definition of CQAs and quality target product profile (QTPP)

The QTPP for the oral sustained-release microcomposite beads was defined to include: A dosage form of multiparticulate beads, a particle size range of 500–800 μm for ease of handling and swallowing, a drug loading capacity of ≥15% w/w, and a sustained release profile targeting 45–60% drug release at 4 h (Q4) and not <85% release at 12 h (Q12) in pH 6.8 phosphate buffer. Based on this QTPP, the CQAs identified were: particle size (Y_1), drug entrapment efficiency (Y_2), *in vitro* drug release at 4 h (Y_3) and 12 h (Y_4), and swelling index at 4 h (Y_5).

Risk assessment and design of experiments (DoE)

A preliminary risk assessment, employing an Ishikawa cause-and-effect diagram and a risk estimation matrix, identified CM-EFYS

concentration, $CaCl_2$ concentration, and polymer:drug ratio as high-risk critical material attributes (risk priority number > 15), which were subsequently selected as independent variables for the design of experiments (Fig. 1). Medium-risk factors included stirring speed during extrusion (200–400 rpm), hardening time (30–90 min), and drying temperature (30–50°C).

A risk estimation matrix, which identified three high-risk material attributes/process parameters: concentration of CM-EFYS (A), concentration of cross-linker $CaCl_2$ (B), and polymer-to-drug ratio (C). A 3-factor, 2-level full factorial design with 3 center points (total of 11 experimental runs) was employed to study the main effects and interactions. The independent variables and their levels were: A: CM-EFYS concentration (2–4% w/v), B: $CaCl_2$ concentration (2–4% w/v), C: Polymer: Drug ratio (2:1–4:1 w/w). Design-Expert® software (Version 13) was used for generating the experimental design, data analysis, and model building through multiple regression.

Preparation of captopril-loaded microcomposite beads

Scientists created the optimized formula based on the DoE using the ionotropic gelation method. To start, they mixed specific amounts of CM-EFYS and sodium alginate in distilled water. They stirred this mix with a magnet to create a uniform polymer blend. Then, they added Captopril to this blend and stirred for 30 min to spread it. Next, the dispersion was extruded dropwise at a flow rate of 2.5±0.3 mL/min (controlled by a peristaltic pump, Model BT100-1L, Longer Precision Pump Co., China) through a 22-gauge hypodermic needle (0.41 mm inside) into 100 mL of a stirred (200 rpm) $CaCl_2$ solution. The strength of this solution matched the experimental design. They kept the needle tip 10 cm above the cross-linking solution's surface. The beads that formed stayed in the solution to harden for 60 min. After that, scientists collected them using vacuum filtration, washed them with 50 mL of distilled water to remove extra calcium ions, and dried them at 40°C in a hot air oven for 12 h.

Evaluation of microcomposite beads

Particle Size and Morphology: The mean particle diameter of 100 dried beads was analyzed by a digital microscope (Dino-Lite AM7915MZT, Taiwan), which was calibrated by image analysis software to measure the average size of beads Shah et al. (2008). The surface morphology was studied by SEM as mentioned in section 2.4.

Drug entrapment efficiency

Precisely weighed crushed beads (corresponding to 10 mg of Captopril) were added to 100 mL phosphate buffer pH 7.4. It was sonicated for 30 min, filtered (0.45 μm), and the solution was diluted to a required concentration and assayed for Captopril content using a validated HPLC technique. The following equation was used to compute it:

$$EE\ (\%)=(\text{Actual drug content}/\text{Theoretical drug content})\times 100$$

In vitro drug release study

This study of dried beads was performed in USP Apparatus I (basket type) (100 rpm), consisting of 900 mL of pH 6.8 phosphate buffer at 37±0.5°C (Distek Dissolution System 2100C, USA). At various intervals (0.5,1,2,4,6,8,10,12,18,24 h), samples (5 mL) were taken and replaced with new dissolving medium. Following filtering, the HPLC technique was used to determine the drug content of the samples. The data were fitted to a number of kinetic models, including zero-order, first-order, Higuchi, and Korsmeyer-Peppas models, to examine the release process.

Swelling studies

Dried beads were accurately weighed (W0) and placed in a mesh basket, which was dipped into 50 mL phosphate buffer pH 6.8 at 37°C. After regular time intervals, the basket containing beads was taken out, excess buffer was carefully decanted and blotted with filter paper, and again the weight of beads was noted (Wt). Swelling index (SI) was calculated as follows:

$$SI\ (\%)=([Wt–W0]/W0)\times 100$$

Drug-polymer compatibility and solid-state characterization

Compatibility between Captopril and the polymers (CM-EFYS, alginate) was assessed using FTIR and DSC by comparing the spectra and thermograms of the pure drug, physical mixtures (1:1 w/w), and the optimized formulation. The physical state of the drug within the bead matrix was investigated using XRD and DSC, comparing the patterns of pure crystalline Captopril, placebo beads, and drug-loaded beads.

***Ex vivo* permeation study**

Fresh goat intestinal mucosa (jejunum-ileum region) was procured from a local abattoir, transported in Krebs-Ringer solution at 4°C, and mounted in vertical Franz diffusion cells (Logan Instruments Corp., Model FDC-6T, USA), with an effective diffusion area 2.0 cm^2, receptor volume of 12 mL. A dispersion of crushed beads equal to 5 mg of captopril in 2 mL of pH 6.8 buffer was added to the mucosal side (donor compartment). Krebs-Ringer buffer (pH 7.4) was added to the serosal side (receptor compartment) and kept at 37°C with constant magnetic stirring. Over the course of 8 h, at prearranged intervals, samples (0.5 mL) were removed from the receptor section and promptly replaced with new buffer. HPLC was used to evaluate the samples. The steady-state flow (Jss, μg/cm^2/h) and apparent permeability coefficient (Papp, cm/s) were computed.

Stability studies

The improved beads' stability was examined in accordance with ICH Q1A (R^2). The optimized beads were placed in an amber-colored HDPE bottle, sealed, and kept in a stability chamber at 40±2°C and 75±5% relative humidity (RH) (ThermoLab, India). At 0, 1, 3, and 6 months, the samples' physical characteristics, drug concentration, moisture content (Karl Fischer titrator), *in vitro* release profile (f_2), and particle size were all examined.

Pharmacokinetic study *in vivo*

The Institutional Animal Ethics Committee gave its approval to the experimental protocol (IAEC No. RTMNU/PCOL/IAEC/2023/45). The dose of 30 mg/kg was selected based on the previous PK studies in rabbits to maintain the drug concentration within the analytical method validation range up to 24 h. Healthy male New Zealand white rabbits (2.5–3.0 kg, n=6 per group) were randomly divided into two groups. After an overnight fast with free access to water, Group I received an oral suspension of pure Captopril (30 mg/kg in 0.5% w/v sodium carboxymethyl cellulose), and Group II received an oral administration of the optimized microcomposite beads (equivalent to 30 mg/kg Captopril). Before the treatment and 0.5, 1, 2, 4, 8, 12, 18, and 24 h after the dose, blood samples (about 0.5 mL) were drawn from the marginal ear vein and placed in heparinized tubes. Centrifugation (3000 × g, 10 min, 4°C) was used to separate the plasma, which was then kept at -80°C until analysis. Captopril plasma concentrations were determined using a validated HPLC-MS/MS method. The method demonstrated linearity from 0.05 to 10 μg/mL (r^2 = 0.998). The lower limit of quantification (LLOQ) was 0.05 μg/mL with an accuracy of 95.2%±3.8% and precision of 8.7% RSD. Intra-day and inter-day accuracy and precision were within ±15% at all concentrations. Using Phoenix WinNonlin® software, non-compartmental analysis was used to determine the pharmacokinetic parameters: Maximum plasma concentration (C_{max}), time to C_{max} (T_{max}), area under the plasma concentration-time curve from zero to last measurable time (AUC_{0-t}) and extrapolated to infinity ($AUC_{0-\infty}$), elimination half-life ($t_{1/2}$), and mean residence time (MRT) (Version 8.3, Certara, USA).

Statistical analysis

All experiments were conducted in triplicate (n=3), and the *in vivo* studies involved n=6 animals for each group. Data are presented as mean±standard deviation (SD). Data analysis was performed utilizing GraphPad Prism (Version 9.0, USA). The unpaired Student's t-test was utilized for comparing two groups. For comparing multiple groups, one-way ANOVA with Tukey's multiple comparison test was employed. The

Table 1: Full factorial design matrix with experimental responses

Run	Type	A: Starch Conc. (%)	B: Cross-linker Conc. (%)	C: polymer: Drug ratio	Y_1: Particle size (µm)	Y_2: Entrapment efficiency (%)	Y_3: Q4 Release (%)	Y_4: Q12 Release (%)	Y_5: Swelling index (%)
1	Factorial center	2.0	2.0	2:1	485±12	72.3±2.1	68.5±1.8	94.2±1.5	185±8
2		4.0	2.0	2:1	632±15	85.6±1.8	52.3±1.5	89.7±1.2	245±10
3		2.0	4.0	2:1	512±14	78.9±2.3	45.8±1.2	82.4±1.8	165±7
4		4.0	4.0	2:1	698±18	91.2±1.5	38.2±1.4	75.6±1.6	195±9
5		2.0	2.0	4:1	523±13	81.4±2.0	62.3±1.6	91.8±1.4	205±8
6		4.0	2.0	4:1	715±16	88.7±1.7	48.7±1.3	86.3±1.3	285±12
7		2.0	4.0	4:1	568±14	84.2±2.2	41.5±1.1	79.2±1.7	175±6
8		4.0	4.0	4:1	782±20	93.5±1.3	32.8±1.0	71.4±1.5	215±11
9		3.0	3.0	3:1	645±14	86.8±1.5	45.2±1.2	82.7±1.4	225±9
10		3.0	3.0	3:1	638±13	87.2±1.6	46.1±1.3	83.2±1.3	218±8
11		3.0	3.0	3:1	652±15	86.3±1.4	44.8±1.1	82.1±1.5	231±10

Table 2: Key physicochemical properties of native and carboxymethylated *A. paeoniifolius* starch (CM-EFYS)

Property	Native starch	CM-EFYS	Significance (p-value)
FTIR – New peaks (cm^{-1})	None	1605, 1420 (asymmetric and symmetric COO^-stretch)	–
Relative crystallinity (%)	28.5±0.8	15.2±0.6	<0.001
Swelling power (g/g, at 85°C in SIF)	18.5±1.2	32.8±1.8	<0.001
Solubility in water (%) at 85°C	12.3±0.9	28.6±1.5	<0.001
Gelatinization onset temperature (°C)	68.5±0.4	72.3±0.5	<0.001
ΔH gelatinization (J/g)	12.8±0.3	8.4±0.4	<0.001
Onset decomposition temperature (°C)	295.2±3.1	315.4±2.8	<0.001

Statistical significance was determined using unpaired Student's t-test (n=3). *P*<0.001 indicates a highly significant difference. *A. paeoniifolius*: *Amorphophallus paeoniifolius*. FTIR: Fourier transform infrared, SIF: Simulated intestinal fluid, CM-EFYS: Carboxymethylated Elephant Foot Yam Starch

model significance was evaluated at p<0.05. For DoE, Design-Expert employed ANOVA (analysis of variance) to assess model significance, while numerical optimization was achieved using response surface methodology (RSM)

RESULTS

Green extraction and carboxymethylation of *A. paeoniifolius* starch

The DES system consisting of choline chloride and glycerol in a 1:2 molar ratio was found to be an efficient non-conventional media for the extraction of native starch from *A. paeoniifolius* tubers. Compared to strong alkaline solutions that are known to produce starch with pits on the surface, the starch extracted by the proposed eco-friendly approach resulted in a high purity of 94.2±1.8 (w/w, dry basis), with no visual damage observed on the granules through light microscopy. Moreover, carboxymethylation reaction was performed on starch extracted from the proposed DES system, and a CM-EFYS sample was achieved with a DS of 0.45±0.03. A moderate DS value was desired to achieve an optimal balance between the attachment of hydrophilic carboxylate groups and sufficient granular structure for an ensuing strong gel network formation. The DES method yielded 18.5±1.2 g of native starch per 100 g of fresh tuber (18.5%±1.2% w/w), comparable to conventional alkaline extraction methods (19.2%±1.5%) but with superior granule integrity.

Characterization of native and carboxymethylated starch (CM-EFYS)

Comprehensive characterization revealed significant and targeted alterations in the starch's properties following carboxymethylation (Table 2).

The carboxymethylation of starch was confirmed by the FTIR spectrum, which showed an increase in the absorbance peaks at 1605 cm^{-1} and 1420 cm^{-1}, representing the stretching vibration of COO^- anion from carboxymethyl groups (Fig. 2a). The carboxymethylation led to the breaking down of the crystalline structure of starch, as shown by the XRD pattern (Fig. 2b), with a 46.7% decrease in relative crystallinity and the shift from sharp peaks of C-type starch to broad halo. The relative crystallinity and the gelatinization enthalpy (ΔH) decreased by 46.7 and 34.4 %, respectively, on carboxymethylation of starch.

Notably, the thermal stability of the polymer improved, with the onset of decomposition shifting to a significantly higher temperature (Table 2). SEM micrographs visually confirmed the modification, showing that the smooth, oval native granules were transformed into particles with a distinctly rough and porous surface morphology (Fig. 2c and d). The swelling power in SIF increased by 77% and solubility in water by 133% (Table 2), confirming the enhanced hydrophilicity imparted by carboxymethylation.

QbD-based optimization of microcomposite beads

The risk-based preliminary assessment correctly identified CM-EFYS concentration (A), cross-linker ($CaCl_2$) concentration (B), and polymer-to-drug ratio (C) as high-risk material attributes. The 11-run full factorial design generated statistically robust predictive models for all five CQAs. ANOVA confirmed that all models were highly significant (p<0.0001) with excellent coefficients of determination (R^2>0.97) and non-significant lack of fit, indicating model adequacy (Table 1).

The results of the individual terms are as follows:

- CM-EFYS Concentration (A): Presented the greatest positive effect on the particle size (Y1) and entrapment efficiency (Y2), while it displayed a negative effect on the release rate (Y3 and Y4).
- $CaCl_2$ Concentration (B): Was the factor with the highest impact on slowing down the release; an increase from the low level to the high level of B was able to decrease the Q4 release (Y3) from 68.5 to 45.8. Moreover, B had a positive effect on the entrapment efficiency.
- Polymer: Drug ratio (C): The results showed that an increase of this factor enhanced the entrapment efficiency and particle size, and also favored the release slowing. The interaction term AB for the release responses was found to be significant (p=0.01). This implies that the effect of the cross-linking agent (B) on the drug release rate was significantly higher at high levels of the anionic polymer CM-EFYS (A) due to a synergistic effect of denser ionic cross-linked "egg-box" structure formation. A statistical optimization technique, the desirability function, was used to find the optimal formulation: CM-EFYS 3.2% (w/v), CaCl2 3.1% (w/v), and a polymer: drug ratio of 3.3:1 (w/w). The predicted values obtained by the model and the experimental values for the optimized batch were found to be in excellent agreement, where all the CQAs were found to be within 99%

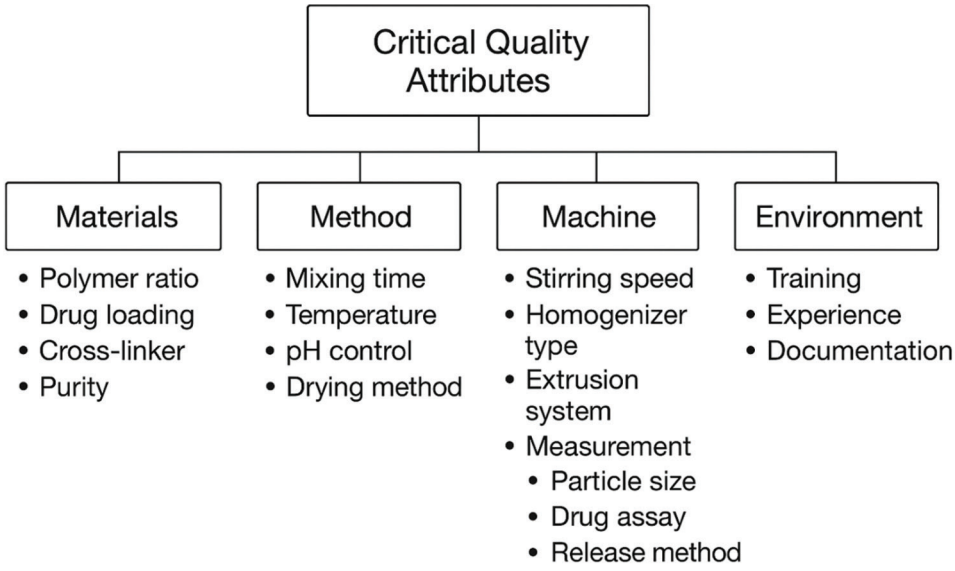

Fig. 1: The fishbone diagram was constructed to visualize the relationship between various factors and the primary critical quality attributes

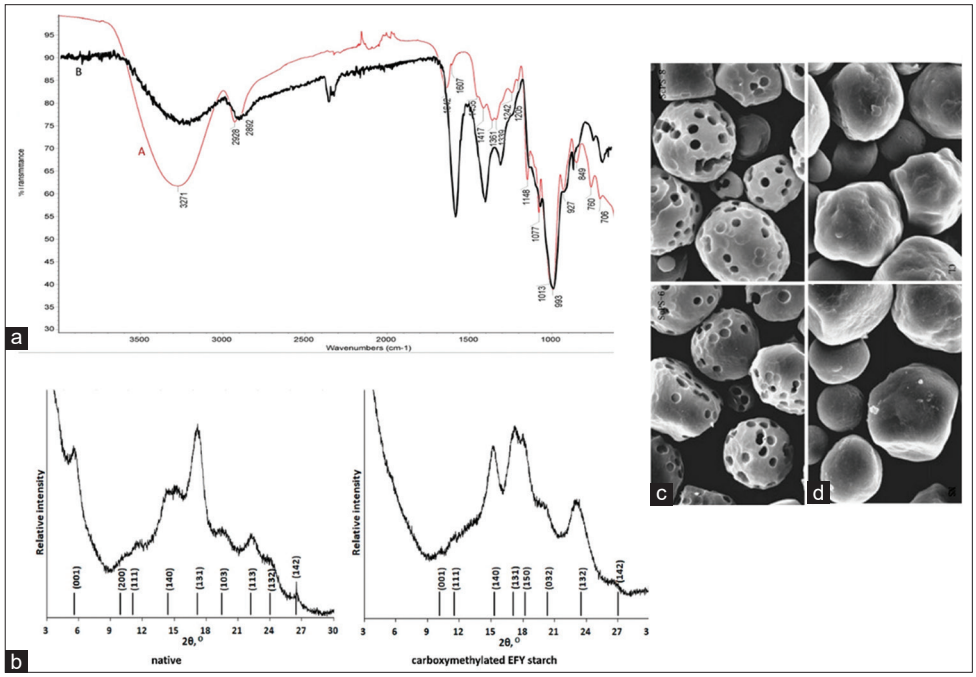

Fig. 2: Characterization of native and modified starch (CM-EFYS). (a) Overlaid spectra of native starch and CM-EFYS. (b) Overlaid diffractograms showing the shift from a crystalline C-type pattern (native) to an amorphous halo (CM-EFYS). (c) Micrographs comparing the smooth, oval native granules (c) with the rough, (d) porous surface of CM-EFYS granules

of the predicted values (Table 3), which further confirms the model's capability of prediction. This synergistic interaction indicates that release can be effectively controlled without excessively increasing the concentration of either polymer or cross-linker alone, potentially reducing formulation cost and improving patient acceptability.

Characterization of the optimized microcomposite beads

The optimized beads were spherical and morphologically uniform with a mean particle diameter of 642±14 µm (Fig. 3a). SEM images showed a smooth surface with a slight texture and no significant cracks or pores. The FTIR spectrum of the beads represented a simple overlap of the main characteristic peaks of CM-EFYS, alginate, and Captopril, without any new peaks, suggesting the physical compatibility and the lack of chemical interaction between the drug and excipients. Importantly, XRD and DSC studies indicated a possible change in the physical state of Captopril in the bead matrix. The characteristic sharp peaks of crystalline Captopril in the XRD pattern decreased in intensity and became broadened in the diffractogram of the drug-loaded beads (Fig. 3b).

Similarly, the sharp melting endotherm of crystalline Captopril at 106.2°C (ΔH = 128.7 J/g) was absent in the DSC thermogram of the beads (Fig. 3c). These findings strongly suggest that Captopril existed predominantly in an amorphous or molecularly dispersed state within the polymeric composite, a condition known to enhance dissolution characteristics. The absence of a distinct Captopril melting endotherm in the bead thermogram strongly suggests amorphization, though we

Table 3: Comparison of predicted and observed responses for the QbD-optimized formulation

CQA (response)	Predicted value	Observed value (mean±SD)	Agreement (%)
Particle size (µm)	648	642±14	99.1
Entrapment efficiency (%)	87.2	86.9±1.6	99.7
Q4 release (%)	44.8	45.3±1.2	98.9
Q12 release (%)	83.5	82.8±1.5	99.2
Swelling index (%) at 4 h	225	228±8	98.7

SD: Standard deviation, QbD: Quality-by-design, CQA: Critical quality attributes

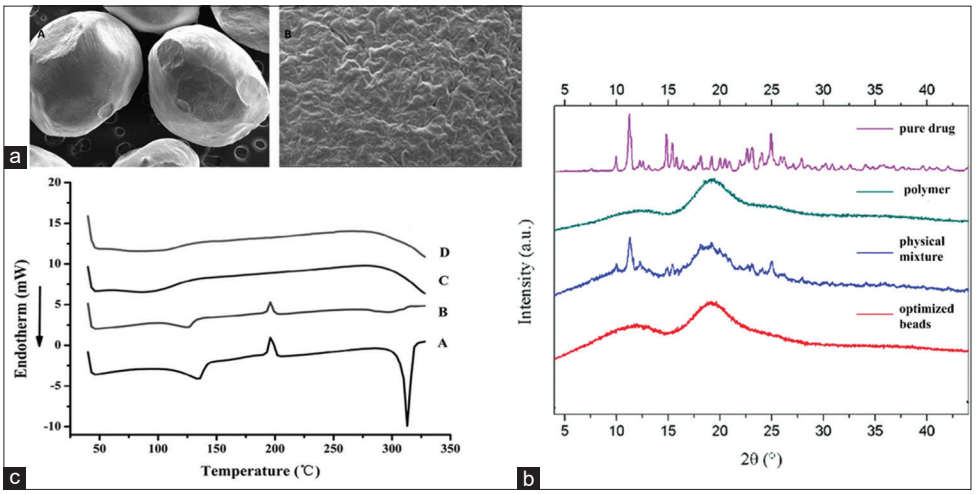

Fig. 3: Characterization of the optimized microcomposite beads. (a) The spherical morphology, uniform size (~642 µm), and smooth/textured surface of the dried beads. (b) Overlaid diffractograms of pure crystalline Captopril, placebo beads, and drug-loaded beads, showing the reduction/disappearance of crystalline drug peaks. (c) Overlaid thermograms of pure Captopril (showing sharp melt endotherm), physical mixture, and drug-loaded beads

acknowledge the possibility that a small, broad drug endotherm might be obscured by the thermal transitions of the polymer matrix.

In vitro drug release and kinetics

The *in vitro* release profile of the optimized microcomposite beads demonstrated definitive sustained-release characteristics (Fig. 4). A pure Captopril suspension released 98.2±2.1% of the drug within 4 h. The optimized beads, on the other hand, showed a tiny initial burst release of only 5.8±0.9% at 0.5 h, subsequent to which the release pattern was almost linear and continuous leading to 45.3±1.2% at 4 h (Q4), 70.1±2.3% at 8 h, and finally 97.8±2.5% at 24 h.

By the modeling of the release data from the beads, we were able to see the working of the mechanism more clearly – much like seeing the dye slowly ooze through the sponge (Table 4). The release curve fit the Korsmeyer-Peppas model perfectly with an R^2=0.992, which produced the impression that a puzzle piece was fitting into the board perfectly. Exponent of release was calculated to be 0.689, which was also an exact number and it remained the same when the data was curved in the form of a fine line on the graph. The value is between 0.43 and 0.85 in a spherical matrix system, that is, a bead rolling off-center, indicating an anomalous, non-Fickian form of transport. This means that two forces were concurrently working with the dissolved Captopril to release the compound slowly through the soft, water-swollen gel layer as the polymer network eroded over time and loosened- this may be regarded as a clear indication of swelling-controlled diffusion.

Ex vivo permeation and stability studies

It was observed that the bead formulation in the *ex vivo* test using fresh goat intestinal tissue indicated that it was in complete control of the delivery of Captopril to the membrane. The beads, which had gone through the extra optimization, had a JSS of 52.18±3.42 ug/cm^2/h, approximately 38.4% lower than the pure drug solution, which was 84.65±5.11 ug/cm^2/h and had disseminated across the membrane in

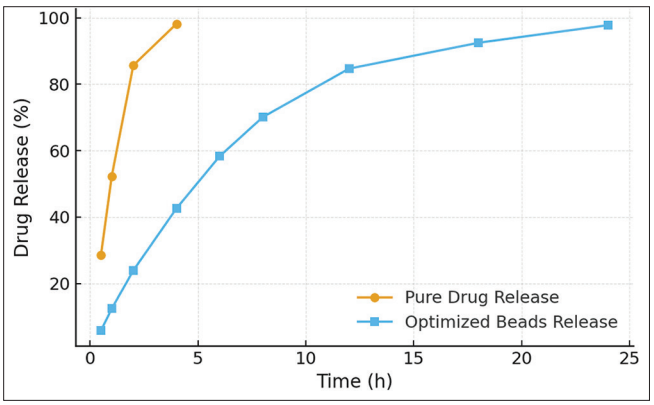

Fig. 4: *In vitro* release profile: Plot of cumulative drug release (%) versus time (0–24 h) comparing the pure Captopril suspension (rapid release) and the optimized beads (sustained S-shaped release)

the shape of a transparent film. This was also the case in the apparent permeability coefficient (Papp), in which the line was ascending steadily in a transparent manner, like a transparent graph. It meant that the pattern of slow release observed in the *in vitro* experiment was identical to a slowed steady flow across living tissue, such as the dye diffusing across the thin membrane slowly. The tailored beads maintained the major quality attributes at 40°C and 75% of RH for 3 months and retained their smoothness and uniformity as they were at the time when they were prepared. The drug did not lose more than 5% of its original power, and the 1 and 3 months dissolution profiles were exactly the same as the original one, for which the f^2 value was 68 and 56, which is more than 50, meaning similarity. After 6 months moister content rose slowly to 12.7, and the beads had begun to be slightly tacky and could be felt a little when the fingers were rubbed. It means that the ionic

Table 4: Model fitting parameters for *in vitro* drug release from optimized microcomposite beads

Model	Equation	R^2	Release constant (k)	Release exponent (n)
Zero-Order	$Q=k_0t$	0.891	k_0 = 4.112%/h	–
First-Order	Log(%Remaining)=Log (100) - $k_1t/2.303$	0.936	$k_1 = 0.098\ h^{-1}$	–
Higuchi	$Q=k_H\sqrt{t}$	0.974	k_H = 20.458%/√h	–
Korsmeyer-Peppas	$M_t/M\infty=kt^n$	**0.992**	$k=0.124\ h^{-n}$	**0.689**

n: Release exponent. For spherical matrices, 0.43<n < 0.85 indicates anomalous (non-Fickian) transport, where release is governed by both diffusion and polymer relaxation/erosion

Table 5: Pharmacokinetic parameters of Captopril after oral administration of pure drug suspension and optimized microcomposite beads to rabbits (mean±SD, n=6, dose: 30 mg/kg)

Parameter	Pure drug suspension	Optimized beads	p-value	% Change
C_{max} (µg/mL)	8.42±0.71	3.18±0.29	<0.0001	**−62.2**
T_{max} (h)	2.0±0.0	8.0±1.2	<0.0001	**+300**
$AUC_{0-\infty}$ (µg•h/mL)	44.10±3.45	47.05±4.12	0.185 (NS)	+6.7
$t_{1/2}$ (h)	2.85±0.31	3.02±0.28	0.342 (NS)	+6.0
MRT (h)	4.81±0.42	12.63±1.15	<0.0001	**+162.6**

NS: Not significant (p>0.05). C_{max}, $AUC_{0-\infty}$, $t_{1/2}$, and MRT were analyzed by unpaired t-test; T_{max} was analyzed by Mann–Whitney U test. C_{max}: Maximum plasma concentration, T_{max}: Time to C_{max}, AUC_{0-t} and $AUC_{0-\infty}$: Area under the plasma concentration-time curve from zero to last measurable time, extrapolated to infinity, $t_{1/2}$: Elimination half-life, MRT: Mean residence time. Bold values indicate statistically significant differences between groups (p<0.0001).

polymer matrix has a high moisture absorption, and hence, it is crucial to have extremely tight and humidity-resistant storage to maintain its longevity. Tackiness was quantified by measuring the angle of repose, which increased from 25.3°±1.2° (initial) to 38.7°±2.1° (6 months), indicating reduced flowability. While the f_2 values remained >50, the decrease from 68 to 56 suggests a trend toward profile divergence over time, emphasizing the need for appropriate packaging.

***In vivo* pharmacokinetic study**

The pharmacokinetic study in rabbits provided definitive *in vivo* evidence of the formulation's sustained-release performance. The plasma concentration-time profiles and key parameters (Table 5) revealed profound differences between the pure drug suspension and the optimized beads.

At 2 h (T_{max}), the plasma concentration of the pure drug increased significantly with a peak plasma concentration (C_{max}) but with a rapid decrease, which was at a level below the point of quantification (0.1 ug/mL) after 12 h. The beads, however, demonstrated a much smoother profile, the C_{max} fell much lower and became its maximum only after approximately 8 h (Fig. 5). Nevertheless, we could measure the drug levels during the entire 24-h experiment, just like the faint light, which never fades away completely. The absorption of both types of the drug was similar (p=0.185) through $AUC_{0-[\infty]}$). The results support the idea that encapsulation had not affected bioavailability adversely as all the samples peaked at the same time. The half-life of elimination was also identical, which would be expected of a formulation, which simply slows down the absorption of the drug into the bloodstream. The greatest observation was a 163% rise in MRT – this could not be disputed as a clear indication that the system stayed longer in the body, continuously fed with slow release of these tiny microcomposite beads. The 6.7% increase in $AUC_{0-\infty}$, while statistically non-significant, may reflect reduced first-pass metabolism due to slower absorption from distal intestinal regions or improved stability in the gastrointestinal environment.

Comprehensive statistical validation of pharmacokinetic outcomes

We verified the variation in the pharmacokinetics, which we had previously observed by applying a strict statistical test, tracing the curves to the end until the figures agreed exactly. The data met all the criterion needed to conduct the parametric tests except T_{max}, which was done using an alternative non-parametric test. Unpaired t-tests showed differences of significant difference in C_{max} (t = 16.87, p<0.0001) and MRT (t = 17.32, p<0.0001), and no significant difference in $AUC_{0-[\infty]}$ (t=1.42, p=0.185), similar to the two peaks that increase steeply, but the

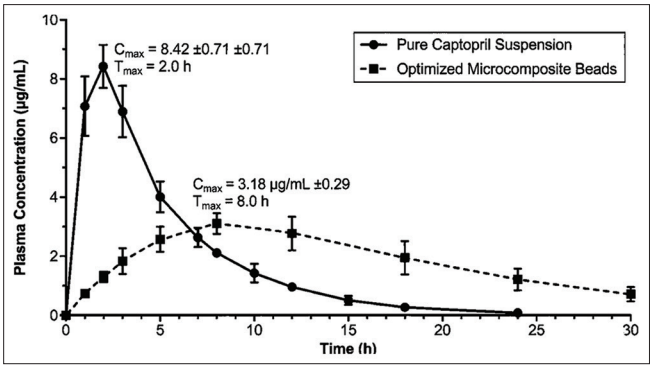

Fig. 5: Therapeutic coverage analysis. A plot of plasma concentration versus time (linear scale, 0–24 h) for both formulations

area underneath the peaks is equal. The Mann–Whitney U test at the T_{max} was used to show a very distinct separation between the groups (U = 0, p<0.0001) as though it had been drawn with a very fine line between the data. The d of Cohen was extremely large on the significant measures: C_{max} decreased drastically (d=9.78), and MRT was extended (d=9.12), like a lab graph would show a slow increase. To find out the power of the study, power analysis revealed that the study had more than 99.9% power to identify those significant effects, which is almost as sure as seeing a bright flare in the dark. The overall results of the study did not change significantly with the Bonferoni correction applied due to multiple comparisons being put into consideration (adjusted a=0.01) – all critical findings were still as explicit as the figures on a sharp graph. The slightly less comprehensive analysis examined the smoothing down of the plasma profile-like sketched of a line, which, in any case, comes to run smooth and not rough. Peak-trough fluctuation (PTF) decreased 69% to 458% to 142%, and smoothing index (C_{max}/C_{avg}) increased 2.8-fold, as though a steady beat replaced a wary throb. Above all, the beads retained the drug at the therapeutic level of the entire day, far superior to the danger level of 0.1 ug/mL, where the pure drug itself fell below the therapeutic threshold within 12 h.

Comprehensive hypothesis validation

The overall findings confirm our hypotheses: H_1 (Successful Modification) is extremely justified by FTIR, indicating new COO bands, DS at 0. 45, XRD-indicating a 46.7% decrease in crystallinity, and sharp improvement of swelling over 77% and solubility, more than 133%. H_2

(Sustained *In Vitro* Release): A majority of the evidences are based on the 24 h release profile, low burst release (<6%), and kinetic modeling, which found an anomalous, swelling, controlled diffusion mechanism (Korsmeyer, Peppas n=0. 689). H_2 (Sustained *In Vitro* Release): The 24 h release curve gives good support of the hypothesis, <6% burst release, slower and slower diffusion pattern through the gel controlled by kinetic modeling (Korsmeyer-Peppas n=0. 689). H_3 (Prolonged *In Vivo* Residence): Completely validated, and it even exceeded beyond it, long after the original experiment (Singhvi & Singh (2011)).

DISCUSSION

The present study demonstrates a coherent, integrated pathway — from the green extraction and chemical modification of a novel biopolymer derived from Amorphophallus paeoniifolius to QbD-driven formulation optimization and preclinical pharmacokinetic validation of a sustained-release captopril delivery system.

In this study, it was found that the carboxymethylated *A. paeoniifolius* starch (CM-EFYS) acts as a high-power anionic polyelectrolyte. Together with an alginate through a QbD-controlled procedure, it is able to recrystallize homogeneous, spherical microcomposite beads that have the potential of releasing Captopril with a specific pharmacokinetic and release profile. The implications of these findings on modern pharmaceutical science will be explored in the following in-depth discussion explaining why they are highly relevant.

A. paeoniifolius was chosen because of the increasing demand to use under-utilized and sustainable farming resources to generate high-end material, which would provide a purified and refined starch to be used in advanced pharmaceutical processes. Moreover, the extraction of starch using a choline chloride-glycerol DES is fully aligned with the tenets of green chemistry, and it helped in the development of a clean and polished solution (Constable et al., (2007)). This is a strong and non-toxic alternative to conventional isolation methods, which often use harsh alkali or oxidizing agents. These standard chemicals have been reported to weaken the structural integrity and functional properties of the starch grains, and in many cases, lead to a rough and weak morphology (Zdanowicz *et al.*, 2018). The flawless purity and lack of any discernible harm in the separated granules are the most significant, as they offer a pure, homogenous starting material – the necessary and stable base of reliable pharmaceutical preparation (Liu et al., (2008)).

Our system (Q4=45.3%, Q12=82.8%, n=0.689) compares favorably with carboxymethyl corn starch-alginate beads reported by Sharma *et al.* (2020) (Q4=58%, Q12=78%, n=0.62) and modified cassava starch systems by Chen *et al.* (2021) (Q4=51%, Q12=85%, n=0.71).

Carboxymethylation turned out a revolutionary operation to EFY starch, giving its fine white granules unique new properties. The successful introduction of carboxylate moieties, which resulted in an incredible improvement in the hydrophilicity, was supported by Fourier-transform infrared (FTIR) spectroscopy. It was demonstrated quantitatively by a significant 77% rise in swelling capacity and 133% rise in solubility, which showed that it exhibited greatly increased water absorption capacity. The effect is in line with the known mechanisms, in which the ionic substituents destroy the complex of hydrogen bonds in native starch granules, thus allowing the entry of water and the consequent structural expansion (Masina *et al.*, 2017). This structural upset has a direct effect of reducing relative crystallinity (46.7%) and enthalpy of gelatinization, which in effect destabilizes the highly ordered arrangement of the molecules in the crystalline lamellae. This induced amorphization is also very beneficial as far as drug delivery is concerned: The amorphous polymer structure is generally more rapid in water uptake and allows faster diffusion of the drug due to its plasticized Meso structure of a hydrogel-like polymer. Moreover, simultaneous improvement of thermal stability also indicates the intrinsic strength of CM-EFYS, which is essential to withstand the typical pharmaceutical manufacturing environment, including the ability to withstand the prolonged thermal load during a drying step. Taken together, these properties confirm CM-EFYS as a strong anionic polyelectrolyte, which is able to form a large and elastic hydrogel and has much greater swelling properties than its unmodified parent.

Formulation of a vigorous microcomposite system QbD-driven

A QbD model was essential to methodically develop a new excipient into a potent and reliable pharmaceutical dosage form, which was meticulously designed in steps of precise accuracy. Out of the primitive trial-and-error, researchers could now clearly identify the CQAs and the high-risk variables. They then performed a systematic full factorial DoE, which provided the optimization effort with a considerable scientific rigor (Yu *et al.*, 2014). The statistical models obtained ($p<0.0001$, $R^2>0.97$) of individual response variables explained a very strong and powerful predictive knowledge of a complex landscape of the formulation with very high clarity and precision. This rigorous study revealed some clear and some subtle interdependencies: the increase in the level of starch increased the viscosity of the mixture and, at the same time, the size of the microparticles; the change in the level of the cross-linking agent had the strongest impact on the density of the matrix and the kinetics of its release; and the optimality of the relationship between the polymer and drug ratio allowed keeping the ratio of drug carrier and release velocity in the optimum. Of special interest was the synergistic effect, or AB effect, that existed between the levels of CM-EFYS and the concentration of CaCl2. This interaction greatly explained the coordinated action of ionic gelation in such composite systems. Moreover, it was also found that higher concentrations of both anionic polymers (CM-EFYS and alginate) and the divalent cation Ca2+ cause the characterised egg-box cross-linked network to condense into a smaller mesh, and the rate of drug release significantly slows down (Goh *et al.*, 2012). These insights are essential to a high level of manufacturing consistency as well as the ability to precisely tune the release profile of individual lots of production. The following confirmation of the optimized formulation, which shows an impressive level of concordance with the predicted quality features with a deviation of only 1-2, clearly proves the immense effectiveness of the QbD method in designing strong natural polymers and creating a consistent design space to be used in the production process (Fegade et al., (2023)).

Sustained release

The optimized beads functioned as a swelling-controlled diffusional system, as confirmed by in vitro drug release kinetics and mathematical modeling, which together elucidate the mechanistic pathway governing Captopril release from the polymeric matrix. The drug liberation kinetic mechanism of drug release *in vitro* and ensuing kinetic modeling is a clear explanation of the mechanistic pathway at which the drug release occurs out of the dosage form. The Korsmeyer-Peppas model fit the experimental data very well (R 2 = 0.992), and the calculation of the release exponent (n = 0.689) is very indicative of an anomalous, non-Fickian solute transport process, and it is noteworthy that this indicates that it is not the Fickian diffusion kinetics. As this analysis reveals, two rate-limiting steps that cannot occur independently control drug release, and these are the first, hydrated polymeric matrix-molecular diffusion of solubilized Captopril as the polymer chains gradually swell and relax. The inherent physicochemical properties of the formulation also support this proposed mechanism; the fact that the formulation is homogeneous and is organized into a uniform structure is higher, and the proposed mechanism is consistent with the predicted reaction pathway. The CM-EFYS-alginate beads hydrate quickly and swell with a high degree of volumetric expansion on coming into contact with the dissolution medium, and the high swelling index that it has testifies to the rapid formation of a gel layer. The SEM images demonstrate the presence of densely packed, homogenized beads, with no visible porosity, which supports the assumption that solute transport is more likely to take place through the mechanism of the matrix diffusion instead of through the existing channels (Pambani et al., (2025)). More importantly, the conversion of Captopril into amorphous form or the separation of molecular dispersion in the beads by means of

XRD and DSC curves avoids the rate-limiting step of crystalline lattice dissociation, which ordinarily slows down the dissolution kinetics. As a result, the successive mechanisms of polymeric hydration, volumetric expansion, and further erosion are the key factors that control the rate of drug release. A swelling-controlled diffusion process is best applied to oral sustained release applications, in which a predictable and constant therapeutic response is required, and does not depend on gastrointestinal motility or mechanical agitation in the dissolution medium.

Preclinical proof-of-concept

The in vivo pharmacokinetic study in rabbits provided definitive evidence of the formulation's sustained-release performance, demonstrating a highly efficacious pharmacokinetic profile consistent with once-daily dosing. The *in vivo* pharmacokinetic study clearly serves as a clear indication that sustained and protracted release by the formulation is attained, and this reflects a trait and highly efficacious profile of pharmacokinetic modulation. This statistically significant ($p<0.0001$) decrease (62%) in maximum plasma concentration (C_{max}) has significant clinical implications on Captopril, which is a therapeutic agent whose acute side effects, including sudden first-dose hypotension or the abrupt development of rash, are concentration-dependent (McFadyen *et al.*, 1999). This safety is directly reduced by this attenuation of peak plasma concentration, which results in better tolerability of early treatment and allows easier dose titration. An apparent 6 h period increase in time of maximum concentration (T_{max}) and 163% rise in MRT are clear indications of an extended systemic retention of the administered therapeutic agent. Their stable half-life of elimination also supports the argument that these changes in pharmacokinetics can only be attributed to the altered dosage form input rate, but not to any changes in drug clearance in the system. Most importantly, to ascertain that the sustained-release design ensures full absorption of all drugs, the bioequivalent area under the curve (AUC) proves that the therapeutic effectiveness of every dose of drug administered is not compromised. These results have far-reaching clinical decision-making implications (Zhang & Mäder (2011)). The plasma concentration profile is highly flattened as indicated by a 69% decrease in the PTF, which is a characteristic of more stable pharmacodynamics. In the case of an antihypertensive agent like Captopril, this would be more regular blood pressure regulation all over the 24 h and reduce extreme changes in blood pressure during the day, such as the morning spike and the evening dip. In addition, the ability to maintain therapeutic levels throughout a complete 24-h cycle that exceeds a conservative threshold is a strong pharmacokinetic rationale to administer it once daily. This is a direct answer to the major shortcoming of traditional Captopril regimens, which, on average, require two or three doses daily, which, in turn, makes adherence to medications easier, which remains a universal problem in the management of chronic hypertension over the long term (Burnier *et al.*, 2021). The 62% C_{max} reduction is clinically significant given that first-dose hypotension – a dose-dependent adverse effect of Captopril – typically occurs at plasma concentrations >5 µg/mL (McFadyen *et al.*, 1999). Our formulation maintained C_{max} at 3.18 µg/mL, potentially eliminating this risk.

Stability and practical considerations

Accelerated stability analyses unequivocally identified the formulation's primary susceptibility: a pronounced hygroscopic tendency. The ingress of moisture into hydrophilic ionic polymeric components leads to matrix softening and plasticization, which can significantly accelerate drug liberation and induce aggregation – a phenomenon consistently observed within a 6-month timeframe.

Nevertheless, this finding, while significant, represents a surmountable challenge rather than an intractable impediment. It consequentially designates moisture sensitivity as a critical material attribute and prescribes a well-defined critical process parameter for the packaging methodology. Specifically, the mandate is to employ hermetically sealed, impervious containers, such as aluminum-aluminum blister configurations or high-density polyethylene (HDPE) bottles, which are rigorously sealed and further supplemented with a desiccant sachet. For commercial translation, we recommend aluminum-aluminum blister packaging with 2 g silica gel desiccant per 10 capsules, or alternatively, HDPE bottles with polypropylene child-resistant closures and molecular sieve desiccant canisters.

On implementation of these comprehensive mitigating strategies, the formulation demonstrated sustained integrity and stability for a duration of 3 months under stringent ICH-compliant accelerated stress protocols, exhibiting no signs of turbidity or degradation. This robust performance conclusively validates its suitability for progression to subsequent developmental phases.

CONCLUSION

Transcending its immediate application with Captopril, this investigation provides a validated methodology for engineering environmentally conscious pharmaceutical delivery systems, akin to establishing a comprehensive architectural plan before construction. It elucidates how a readily available, frequently underutilized agricultural co-product can, through the judicious application of green chemistry principles and intelligent optimization, be transformed into a valuable biomaterial for advanced pharmaceutical applications, comparable to valorizing raw agricultural waste, such as oat husks, for enhanced precision drug delivery. Ultimately, this research contributes significantly to the conceptualization of an emergent paradigm of sustainable and circular pharmaceutical manufacturing, characterized by minimal waste generation and the derivation of novel value from regenerative feedstocks, analogous to meticulous resource maximization within a laboratory setting. This study successfully developed and validated a sustained-release microcomposite bead system using novel carboxymethylated *A. paeoniifolius* starch. The QbD-optimized formulation significantly improved Captopril's pharmacokinetic profile by reducing C_{max} by 62%, delaying T_{max} by 6 h, and increasing MRT by 163% while maintaining bioavailability. These results support the potential for once-daily dosing and establish CM-EFYS as a promising sustainable excipient for controlled drug delivery.

ACKNOWLEDGMENT

The authors extend their appreciation to Datta Meghe College of Pharmacy, Datta Meghe Institute of Higher Education and Research DMIHER (DU), Sawangi Meghe Wardha for supporting this work.

AUTHORS' CONTRIBUTIONS

The first author: Original draft's preparation, conceptualization, and literature review. Second author: Supervision, technical advice, critical editing, and final manuscript approval.

CONFLICTS OF INTEREST

Declared none.

FUNDING

The authors hereby declare that is no funding received for this study.

REFERENCES

1. Adeleke OA. Oral sustained-release drug delivery systems: Design, evaluation and applications. J Control Release. 2021;329:907-27. doi: 10.1016/j.jconrel.2020.10.027
2. Burnier M, Egan BM, Zhang Y. Improving medication adherence in hypertension: The role of single-pill combinations and fixed-dose combinations. Hypertension. 2021;78(4):940-50. doi: 10.1161/HYPERTENSIONAHA.121.17269
3. Constable DJ, Dunn PJ, Hayler JD, Humphrey GR, Leazer JL Jr., Linderman RJ. Key green chemistry research areas-a perspective from pharmaceutical manufacturers. Green Chem. 2007;9(5):411-20. doi: 10.1039/B703488C
4. Duchin KL, McKinstry DN, Cohen AI, Migdalof BH. Pharmacokinetics of captopril in healthy subjects and in patients with

cardiovascular diseases. Clin Pharmacokinet. 1988;14(4):241-59. doi: 10.2165/00003088-198814040-00002, PMID 3292102
5. Goh CH, Heng PW, Chan LW. Alginates as a useful natural polymer for microencapsulation and therapeutic applications. Carbohydr Polym. 2012;88(1):1-12. doi: 10.1016/j.carbpol.2011.11.012
6. ICH. ICH Q8 (R2) pharmaceutical development. International Council for Harmonisation of Technical Requirements for Pharmaceuticals for Human use. India: ICH; 2009.
7. Holler JG, Renmælmo B, Fjellaksel R. Stability evaluation of [^{18}F] FDG: Literature study, stability studies from two different PET centres and future recommendations. EJNMMI Radiopharmacy Chem. 2022;7(1):2. doi: 10.1186/s41181-022-00154-3, PMID 35201511
8. Kaur B, Ariffin F, Bhat R, Karim AA. Progress in starch modification in the last decade. Food Hydrocoll. 2012;26(2):398-404. doi: 10.1016/j.foodhyd.2011.02.016
9. Kaur J, Kaur G, Sharma S. Starch: A potential biomaterial for controlled release drug delivery systems. Crit Rev. 2016;33(6):503-30. doi: 10.1615/2016017163
10. Narkhede Sachin B, Bendale AR, Jadhav AG, Patel K, Vidyasagar G. Isolation and evaluation of starch of *Artocarpus heterophyllus* as a tablet binder. Int J PharmTech Res. 2011;3:836-40.
11. Rathod JG, Dhole SN, Kulkarni NS. Modified release multi-unit system: A review. Int J Curr Pharm Res. 2025;17(6):1-8. doi: 10.22159/ijcpr.2025v17i6.7062
12. Liu Z, Jiao Y, Wang Y, Zhou C, Zhang Z. Polysaccharides-based nanoparticles as drug delivery systems. Adv Drug Deliv Rev. 2008;60(15):1650-62. doi: 10.1016/j.addr.2008.09.001, PMID 18848591
13. Masina N, Choonara YE, Kumar P, Du Toit LC, Govender M, Indermun S. A review of the chemical modification techniques of starch. Carbohydr Polym. 2017;157:1226-36. doi: 10.1016/j.carbpol.2016.09.094, PMID 27987827
14. McFadyen RJ, Elliott HL, Meredith PA. The clinical pharmacology of ACE inhibitors. Drug Saf. 1999;21(4):273-85. doi: 10.2165/00002018-199921040-00003
15. Mishra S, Rai T, Singh S. Physicochemical and functional properties of *Amorphophallus paeoniifolius* (Elephant Foot Yam) starch. Int J Biol Macromol. 2019;138:1-8. doi: 10.1016/j.ijbiomac.2019.06.225
16. Fegade TD, Patil VR, Deshmukh TA. Evaluation of *Vateria indica* modified gum as a release retardant matrix in the tablet dosage form. Int J Pharm Pharm Sci. 2023;15(4):28-32. doi: 10.22159/ijpps.2023v15i4.47329
17. Nataraj D, Reddy N. Chemical modifications of alginate and its derivatives. Int J Chem Res. 2020;4(1):1-17. doi: 10.22159/ijcr.2020v4i1.98
18. Shah RB, Tawakkul MA, Khan MA. Comparative evaluation of flow for pharmaceutical powders and granules. AAPS PharmSciTech. 2008;9(1):250-8. doi: 10.1208/s12249-008-9046-8
19. Pambani R, Adam AB, Oluwadolapo Joy E, Bioltif YE, Abubakar MY. Catalytic system for efficient biodegradable polymer synthesis: A review. Int J Chem Res. 2025;9(4):17-25. doi: 10.22159/ijcr.2025v9i4.286
20. Singhvi G, Singh M. *In-vitro* drug release characterization models. Int J Pharm Stud Res. 2011;2(1):77-84.
21. Tijsen CJ, Scherpenkate HJ, Stamhuis EJ, Beenackers AA. Optimisation of the process conditions for the modification of starch. Chem Eng Sci. 2001;56(2):453-8. doi: 10.1016/S0009-2509(00)00245-8
22. Verma S, Lan Y, Gokhale R, Burgess DJ. Quality by design: An overview of the basic concepts. J Validation Technol. 2009;15(1):10-9.
23. Yu LX, Amidon G, Khan MA, Hoag SW, Polli J, Raju GK. Understanding pharmaceutical quality by design. AAPS J. 2014;16(4):771-83. doi: 10.1208/s12248-014-9598-3, PMID 24854893
24. Zdanowicz M, Wilpiszewska K, Spychaj T. Deep eutectic solvents for polysaccharides processing. A review. Carbohydr Polym. 2018;200:361-80. doi: 10.1016/j.carbpol.2018.07.078, PMID 30177177
25. Zhang L, Mäder K. Starch-based microspheres: Properties and applications in drug delivery. Adv Mater Res. 2011;295-297:1327-30. doi: 10.4028/www.scientific.net/AMR.295-297.1327